

# **National Oceanography Centre, Southampton**

## **Research & Consultancy Report No. 85**

Notes on a I-D model of  
continental shelf resonances

D J Webb

2011

National Oceanography Centre, Southampton  
University of Southampton, Waterfront Campus  
European Way  
Southampton  
Hants SO14 3ZH  
UK

Author contact details  
Tel: +44 (0)23 8059 6199  
Email: [djw@soton.ac.uk](mailto:djw@soton.ac.uk)

## *DOCUMENT DATA SHEET*

<i>AUTHOR</i> WEBB, D J	<i>PUBLICATION</i> <i>DATE</i> 2011
<i>TITLE</i> Notes on a 1-D model of continental shelf resonances.	
<i>REFERENCE</i> Southampton, UK: National Oceanography Centre, Southampton, 12pp. (National Oceanography Centre Southampton Research & Consultancy Report, No. 85) (Unpublished manuscript)	
<i>ABSTRACT</i> <p>This paper reviews earlier work and provides new results from a one-dimensional model of the scattering of a tidal wave by a continental shelf. When the continental shelf is many wavelengths wide, a large fraction of the incident tidal energy can propagate from the deep ocean onto the shelf. In contrast when there is a nearby coastline most of the energy is reflected unless the shelf approximately <math>1/4</math>, <math>3/4</math>, <math>5/4</math> etc wavelengths wide and has a suitable amount of frictional damping.</p> <p>The properties of the reflection coefficient are investigated. It is shown that it can be treated as a function of complex angular velocity, strong absorption of tidal energy being associated with nearby poles in the complex angular velocity plane. Physically the poles correspond to decaying shelf modes, their real component depending primarily on the geometry of the region and their imaginary components to their rate of decay. The latter depends on both the bottom friction, acting on the shelf, and on the radiation of energy back into the deep ocean. It is also shown that the reflected wave can be zero when the two are equal and that this can occur for physically realistic values for the depths, shelf width and bottom friction coefficient. Shelf resonances thus provide a classic example of impedance matching.</p> <p>The amplitude and phase of the reflected wave are also investigated and it is found that when plotted in a suitable manner as a function of real angular velocity they produce a characteristic loop as each resonance is passed. Such loops can be useful for identifying nearby resonances in model studies and in data from the real ocean.</p>	
<i>KEYWORDS</i>	
<i>ISSUING ORGANISATION</i> <b>National Oceanography Centre, Southampton University of Southampton, Waterfront Campus European Way Southampton SO14 3ZH UK</b>	

# Notes on a 1-D Model of Continental Shelf Resonances

David J. Webb

National Oceanography Centre, Southampton SO14 3ZH, U.K.

## Abstract.

This paper reviews earlier work and provides new results from a one-dimensional model of the scattering of a tidal wave by a continental shelf. When the continental shelf is many wavelengths wide, a large fraction of the incident tidal energy can propagate from the deep ocean onto the shelf. In contrast when there is a nearby coastline most of the energy is reflected unless the shelf approximately  $1/4$ ,  $3/4$ ,  $5/4$  etc wavelengths wide and has a suitable amount of frictional damping.

The properties of the reflection coefficient are investigated. It is shown that it can be treated as a function of complex angular velocity, strong absorption of tidal energy being associated with nearby poles in the complex angular velocity plane. Physically the poles correspond to decaying shelf modes, their real component depending primarily on the geometry of the region and their imaginary components to their rate of decay. The latter depends on both the bottom friction, acting on the shelf, and on the radiation of energy back into the deep ocean. It is also shown that the reflected wave can be zero when the two are equal and that this can occur for physically realistic values for the depths, shelf width and bottom friction coefficient. Shelf resonances thus provide a classic example of impedance matching.

The amplitude and phase of the reflected wave are also investigated and it is found that when plotted in a suitable manner as a function of real angular velocity they produce a characteristic loop as each resonance is passed. Such loops can be useful for identifying nearby resonances in model studies and in data from the real ocean.

## 1 Introduction

Webb (1976) investigated the absorption of tidal energy by a continental shelf and showed that under the right conditions

*Correspondence to:* D.J.Webb (djw@soton.ac.uk)

continental shelf resonances may completely absorb incident energy. The study made use of a 2-D barotropic tidal model but in an appendix to the paper, the Green's Function of a simpler 1-D model was briefly discussed. The 1-D model was also used to in a later review article to illustrate the key physical and mathematical concepts (Webb, 1982), but again the amount of detail given was limited.

Following the original study, Buchwald (1980) simplified the problem in a different way by considering the reflection of Poincaré waves which approached the shelf at an angle. One important result of this study was that it showed that complete absorption of tidal energy occurred for a single value of the friction parameter. The approach using Poincaré waves was further developed by Middleton & Bode (1987) and Das & Middleton (1997).

Duff (1970) had previously studied the tides of the Bay of Fundy in terms of resonances and the application to real systems was continued by Greenberg (1979) for the Bay of Fundy, Fong & Heaps (1978) and Heath (1981), for the Bristol Channel, and Huthnance (1980), who explained features of the Brazilian M3 tides in terms of shelf resonances. Other papers discussing shelf resonances include Clarke & Battisti (1997) and Webb (1973).

Up to this stage, raw data on the tides of such regions came primarily from scattered coastal tide gauges, but the groundbreaking study of Cartwright & Ray (1990) provided an important new source of data: accurate global maps of the tides based on satellite altimeter measurements. Egbert & Ray (2001) and Egbert & Ray (2003) used TOPEX/Poseidon satellite data to investigate the global flux of tidal energy and showed that a third of the tidal energy was lost in the deep ocean near mid-ocean ridges and other topographic features. The result helped stimulate further research because the tidal energy then becomes available for mixing in the deep ocean and, as such, is thought to have a significant effect on the global ocean circulation.

The results of Egbert & Ray (2001) also confirmed the

importance of resonant continental shelves. These included the N.W. Australian Shelf, the Patagonian Shelf and the European Shelves. However the authors also found that the Labrador Shelf and Hudson Strait region dissipated over twice the energy previously estimated by Miller (1966). As a result it became one of the most important dissipation regions for tidal energy. It may even be the most important.

O'Reilly, Solvason and Solomon (2005) analysed data from Ungava Bay, a branch of Hudson Strait, and found that the tidal range there can reach 16.8 m, a value similar to that of the resonant Bay of Fundy and Bristol Channel regions. Arbic et. al. (2007) used a numerical model to show that the Ungava Bay-Hudson Strait region has a natural resonance period near 12.7 hours, within or close to the band of the semi-diurnal tides. The exact value is dependent the boundary condition used to match the regional model to the deep ocean, an effect which has been investigated further by Arbic, Karsten & Garrett (2009).

Given the increased interest in the tides and resonances, it appears timely to provide more details and results from the 1-D model discussed by Webb (1976) and Webb (1982). The simplicity of the model means that it can be used to study shelf resonances in ways that are difficult or impossible with normal numerical models. Thus it can be readily used to investigate the complex angular velocity plane, the factors determining their position and they way that they move as the friction and boundary conditions are varied.

The model also shows that if the shelf is infinitely wide, large fraction of the tidal energy can propagate onto the shelf, even when the shelf is only 50 m and the ocean 4000 m deep. The result is only weakly affected by the amount of tidal friction acting on the shelf and the angular velocity of the incident wave.

When the shelf is narrow the energy reflected by the shelf is much larger, except near one of the shelf resonances. The form of the response near a resonances is investigated, confirming the result of Buchwald (1980) that complete absorption of tidal energy occurs at a single value of the friction parameter. Mathematically it is found that the result is essentially inevitable for a linear physical system with analytic solutions. Physically it is shown that complete absorption occurs when the frictional damping and the radiation damping of the shelf modes are equal and that this is possible within the normal range of parameters found on continental shelves. occur. Thus the resonant absorption of tidal energy is a classic example of impedance matching within a physical system.

## 2 The 1-D model

The tides of the ocean are primarily long barotropic waves for which the velocity is independent of depth. Such waves are described by Laplace's tidal equations which in a one-dimension channel where the Coriolis force can be neglected,

become,

$$\begin{aligned}\rho \partial u / \partial t &= -\rho g d\zeta / \partial x + F / h, \\ \partial \zeta / \partial t &= -h \partial u / \partial x.\end{aligned}\quad (1)$$

where  $\zeta$  is the tidal height,  $u$  the velocity,  $\rho$  the density of water,  $t$  time and  $x$  the distance along the channel. The acceleration due to gravity is given by  $g$  and  $h$  is the depth of the channel.  $F$  is the bottom friction, which is assumed to be proportional to the velocity and have the form,

$$F = -\rho \kappa u, \quad (2)$$

where  $\kappa$  is a constant of order  $10^{-3} \text{ ms}^{-1}$ .

In regions where the depth  $h$  is a constant, the equations have progressive wave solutions of the form,

$$\begin{aligned}\zeta &= \zeta_0 \exp(ikx - i\omega t), \\ u &= u_0 \exp(ikx - i\omega t),\end{aligned}\quad (3)$$

where at any given instant the actual tidal height and velocity,  $\zeta_r$  and  $u_r$ , are given by the real part of the expressions. Alternatively they can be considered as being the sum of of their complex equivalents plus the complex conjugates,

$$\begin{aligned}\zeta_r &= \zeta + c.c., \\ u_r &= u_0 + c.c.\end{aligned}\quad (4)$$

Substituting Eqn. 3 in 1,

$$\begin{aligned}-i\omega u &= -ikg\zeta - \kappa u/h, \\ -i\omega \zeta &= -ikh u.\end{aligned}\quad (5)$$

Thus,

$$\begin{aligned}u &= (\omega/(hk))\zeta, \\ k &= (\omega^2 + i\kappa\omega/h)^{1/2}/(gh)^{1/2}, \\ &= (1 + i\beta/\omega)^{1/2} \omega/c,\end{aligned}\quad (6)$$

where,

$$\begin{aligned}c &= (gh)^{1/2}, \\ \beta &= \kappa/h.\end{aligned}$$

$c$  is the wave speed with no bottom friction.  $\beta$  has the dimensions of inverse time and, in terms of the physics, is the inverse decay time of the current field due to friction (eqn 1).

Consider a semi-diurnal tidal wave on a continental shelf with a depth of 50 m and where  $\kappa$  equals  $10^{-3} \text{ ms}^{-1}$ . Then the ratio  $\beta/\omega$  has the value 0.14 and in the equation for the wavenumber can be treated as a small quantity. Thus from Eqn. 7,

$$\begin{aligned}k &= \frac{\omega}{c} \left(1 + i\frac{\beta}{2\omega} - \frac{3}{8}\left(\frac{\beta}{\omega}\right)^2 + O(\beta^3)\right), \\ &= \frac{\omega}{c} + i\frac{\beta}{2c} - \frac{3}{8c\omega}\beta^2 + O(\beta^3).\end{aligned}\quad (8)$$

Thus on a typical continental shelf the real part of the wavenumber is, to a good approximation, linearly dependent

on angular velocity and the imaginary part is independent of the angular velocity.

The same wave in a deep ocean with a depth of 4000 m, will have  $\beta/\omega$  equal to 0.0017. In the rest of this paper we will treat this as being essentially zero and assume that the deep ocean is frictionless.

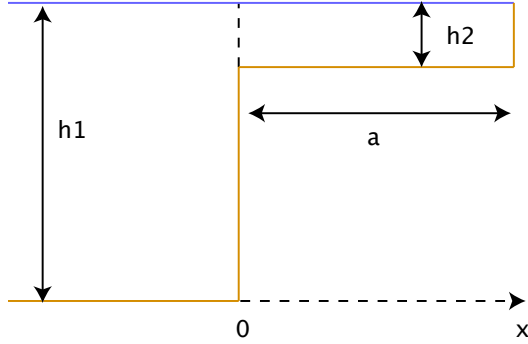


**Fig. 1.** The one-dimensional model of ocean and shelf. The ocean has depth  $h_1$ , the continental shelf depth  $h_2$  and width  $a$ .

### 3 Ocean and Shelf

We apply these equations to the 1-D model of an ocean and continental shelf shown in figure 1. The ocean, which lies along the negative x-axis, is of uniform depth  $h_1$ . The continental shelf has uniform depth  $h_2$  and has a width  $a$ . In the deep ocean the tide is represented by a incident wave of unit amplitude and a reflected wave with coefficient  $R$ .

$$\zeta_1(x) = (\exp(i k_1 x) + R \exp(-i k_1 x)) \exp(-i \omega t). \quad (9)$$

$R$  is a complex number representing the amplitude and phase of the reflected wave.

On the shelf, the tide is also represented by the sum of an incident and reflected wave,

$$\zeta_2(x) = (A_1 \exp(i k_2 x) + A_2 \exp(-i k_2 x)) \exp(-i \omega t). \quad (10)$$

The boundary condition at the coast is that the flux  $h_2 u_2$  is zero. At the shelf edge, the tidal heights,  $\zeta_1$  and  $\zeta_2$ , and the fluxes,  $h_1 u_1$  and  $h_2 u_2$ , must both be equal.

#### 3.1 Ocean and Infinite Width Shelf

Consider first the case where there is no coastline and the continental shelf extends to infinity. There is then no reflected wave on the shelf and the solution there has the form,

$$\begin{aligned} \zeta_2 &= A \exp(i k_2 x - i \omega t), \\ u_2 &= A (\omega / (h_2 k_2)) \exp(i k_2 x - i \omega t). \end{aligned} \quad (11)$$

From the matching conditions at the shelf edge,

$$\begin{aligned} 1 + R &= A, \\ 1 - R &= (k_1/k_2) A. \end{aligned} \quad (12)$$

Solving for the coefficients  $R$  and  $A$ ,

$$\begin{aligned} R &= (1 - k_1/k_2)/(1 + k_1/k_2), \\ A &= 2/(1 + k_1/k_2). \end{aligned} \quad (13)$$

where from equation 7, if  $\beta_2$  is the value of  $\beta$  on the shelf,

$$\begin{aligned} k_1/k_2 &= (h_2/h_1)^{1/2} (1 + i\beta_2/\omega)^{-1/2}, \\ &= (h_2/h_1)^{1/2} (1 - \frac{i\beta_2}{2\omega} + O((\frac{\beta_2}{\omega})^2)). \end{aligned} \quad (14)$$

As  $\beta_2/\omega$  is small, the functions  $R$  and  $A$  are to a first approximation only dependent on the ratio of the depths and are independent of friction or the angular velocity of the incident wave.

#### 3.2 Ocean and Finite Width Shelf

When the shelf has finite width, the boundary condition at the coast gives the relation,

$$h_2(A_1 \exp(i k_2 a) - A_2 \exp(-i k_2 a)) = 0. \quad (15)$$

The solution on the shelf can thus be written,

$$\begin{aligned} \zeta_2 &= A \cos(k_2(x - a)) \exp(-i \omega t), \\ u_2 &= A(i\omega/(h_2 k_2)) \sin(k_2(x - a)) \exp(-i \omega t). \end{aligned} \quad (16)$$

The boundary conditions at the shelf edge become,

$$\begin{aligned} 1 + R &= A \cos(k_2 a), \\ 1 - R &= -i(k_1/k_2) A \sin(k_2 a) \end{aligned} \quad (17)$$

Thus,

$$\begin{aligned} R(\omega) &= \frac{(\cos(k_2 a) + i(k_1/k_2) \sin(k_2 a))}{(\cos(k_2 a) - i(k_1/k_2) \sin(k_2 a))}, \\ A(\omega) &= 2/(\cos(k_2 a) - i(k_1/k_2) \sin(k_2 a)). \end{aligned} \quad (18)$$

Physically the angular velocity  $\omega$  is a real quantity, but it can be treated as a complex number, in which case, in eqns. 13 and 18, the functions  $k_1$ ,  $k_2$ ,  $R$  and  $A$  are all complex analytic functions<sup>1</sup> of  $\omega$ . As is discussed later, the poles of the functions  $R$  and  $A$  correspond to the resonances of the physical system.

<sup>1</sup>The term is used in the physicists' sense in that the functions are smooth and satisfy the Cauchy-Reimann conditions except at poles and branch points in the complex plane. An alternative term is holomorphic.

**Table 1.** Equation 13 results for the diurnal and semi-diurnal tides propagating in an ocean of depth 4000 m and incident on an infinitely wide continental shelf, with differing value of shelf width and friction coefficient. The table gives the wavelengths in the deep ocean and on the shelf, the decay length on the shelf and the values of the reflection coefficient and its square (the fraction of incident energy reflected).

Period (hours)	12				24			
Depth (m)	50		100		50		100	
Friction coefficient	0	0.001	0	0.001	0	0.001	0	0.001
Ocean wavelength (km)	8558	8558	8558	5885	17115	17115	17115	17115
Shelf wavelength (km)	957	955	1353	1352	1914	1896	2706	2700
Shelf decay length (km)		2220		6268		2235		6279
Full solution :								
$ R $	0.7989	0.8002	0.7269	0.7274	0.7989	0.8038	0.7269	0.7286
$ R ^2$	0.6380	0.6402	0.5285	0.5290	0.6380	0.6461	0.5285	0.5309
Eqn. 14 approximation :								
$ R $	0.7763	0.7765	0.6838	0.6839	0.7763	0.7770	0.6838	0.6841
$ R ^2$	0.6028	0.6030	0.4675	0.4677	0.6028	0.6037	0.4675	0.4680

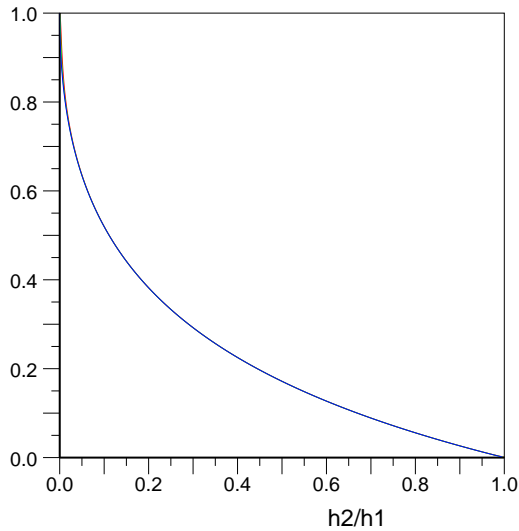


**Fig. 2.** The amplitude of the reflection coefficient  $R$  as an function of  $h_2/h_1$ , for the case (blue line) where the shelf is infinitely wide and there is no friction. For the standard case studied where  $h_2$  is 4000 m and  $h_1$  is 50 m, the ratio equals 0.0125. The zero friction results are plotted on top of the results for friction coefficients of  $10^{-3} \text{ ms}^{-1}$  (green) and  $2 \cdot 10^{-3} \text{ ms}^{-1}$  (red).

## 4 Properties of the Solution

### 4.1 Infinite Width Shelf

When the shelf has infinite width, the functions  $R$  and  $A$  depend primarily on the ratio  $h_2/h_1$  (eqns. 13, 14). Fig. 2 shows the amplitude of  $R(\omega)$  plotted as a function of this ratio for the case where there is no friction either on the shelf or in the deep ocean.

The amplitude is unity when the shelf has zero depth, cor-

responding to perfect reflection, and initially drops off very rapidly as the shelf depth increases. As shown in table 1, the reflected amplitude is 0.79 for the 50 m shelf, when the ratio is 0.0125, and reduces to 0.73 for the 100 m shelf when the ratio is 0.025. The energy flux depends on the square of the amplitude, so the fraction of incident energy reflected is approximately 64% for a 50 m shelf and 53% for a 100 m shelf. Both the reflected amplitude and the flux become zero when the shelf depth equals the depth of the ocean.

The behaviour at small shelf depths can be understood from eqns. 13 and 14. Combining the two equations,

$$R = (1 - \alpha^{1/2}(1 - \frac{i\beta}{2\omega})) / (1 + \alpha^{1/2}(1 + \frac{i\beta}{2\omega})) \quad (19)$$

where,

$$\alpha = h_2/h_1 .$$

If there is no friction on the shelf then  $\beta$  is zero and,

$$R = (1 - \alpha^{1/2}) / (1 + \alpha^{1/2}) \\ \approx 1 - 2\alpha^{1/2} .$$

Thus,

$$\partial R / \partial \lambda \approx -\alpha^{-1/2} . \quad (20)$$

As  $\alpha$  tends to zero, the slope of the curve becomes infinitely steep.

Adding a realistic amount of friction to the shelf has only a small effect on the results. In fig. 2 the zero friction solution is plotted on top of solutions for which  $\kappa$  has the values of  $10^{-3}$  and  $2 \cdot 10^{-3} \text{ ms}^{-1}$ . The differences are only visible as the shelf depth tends to zero but even then the differences remain small.

Specific values are given in table 1. For a shelf depth of 50 m,  $|R|$  equals 0.8002 when  $\kappa$  equals  $10^{-3} \text{ ms}^{-1}$ , only slightly larger than the value of 0.7989 for the frictionless case. Doubling the friction (or equivalently halving the angular velocity, i.e. for the diurnal tide), doubles the value of  $\beta$  but only

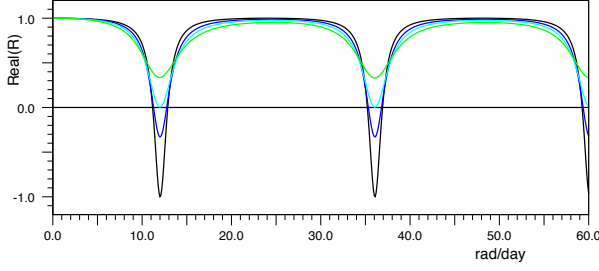


**Fig. 3.** The real component of the reflection coefficient  $R$  as a function of angular velocity  $\omega$  (radians/day), for four values of the friction coefficient  $\kappa$  (eqn. 1). The values of  $\kappa$  are:  $0 \text{ ms}^{-1}$  (black),  $5 \cdot 10^{-4} \text{ ms}^{-1}$  (dark blue),  $10^{-3} \text{ ms}^{-1}$  (light blue),  $2 \cdot 10^{-3} \text{ ms}^{-1}$  (green).

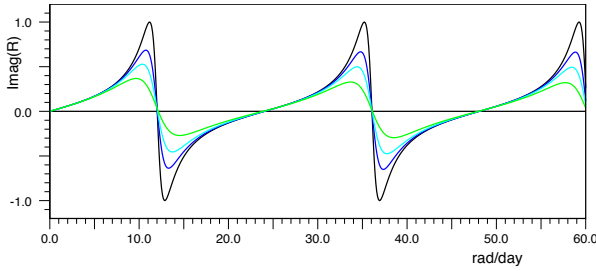


**Fig. 4.** The imaginary component of the reflection coefficient  $R$  as a function of angular velocity  $\omega$ , for four values of the friction coefficient  $\kappa$  (eqn. 1). Colours as in fig. 3.

increases  $|R|$  to 0.8038. For the case where the shelf depth is increased to 100 m, the effect of friction is even smaller.

In conclusion the results of this section show that an infinitely wide shelf will reflect around half to two-thirds of the incident energy. They also show that for practical values of friction, shelf depth and angular velocity; the ratio of depths  $\alpha$  is small and the friction term  $\beta$  can be treated as if it is zero. As a result the reflected wave amplitude is effectively independent of the angular velocity, and it can be represented to a good approximation by a perturbation expansion, such as eqn. 20 with  $\beta$  set to zero.

Although no realistic shelf can be really infinitely wide, the results of this section may be good approximations for a shelf that is wide enough and has sufficient friction that the wave returning to the shelf edge has negligible amplitude. In practice however, with a few exceptions like Hudson Bay, continental shelves are much narrower than this and the effects of reflection are important.

#### 4.2 Finite Width Shelf

The results for a more realistic shelf, with a width of 250 km, are shown in figs. 3 and 4. The figures show the real and imaginary components of the reflection coefficient  $R$  as a

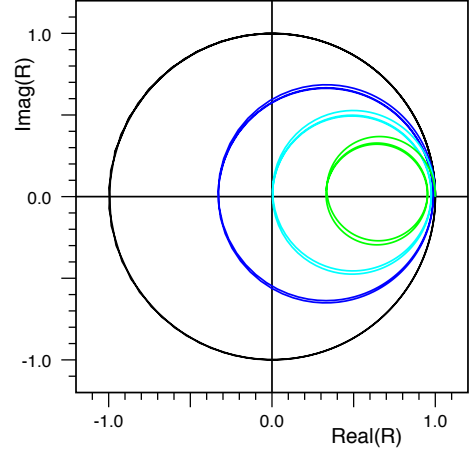


**Fig. 5.** The locii of the reflection coefficient  $R$ , plotted in the complex plain as an function of angular velocity  $\omega$ , for four values of the friction coefficient  $\kappa$  (eqn. 1). Colours as in fig. 3.

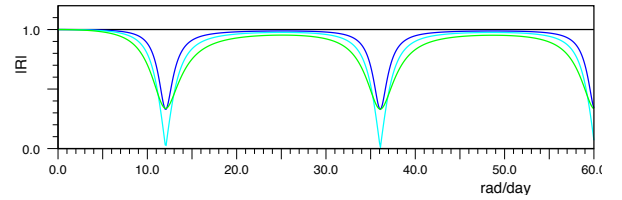


**Fig. 6.** The amplitude of the reflection coefficient  $R$  as an function of angular velocity  $\omega$ , for four values of the friction coefficient  $\kappa$  (eqn. 1). Colours as in fig. 3.

function of the angular velocity for four values of the friction coefficient  $\kappa$ . As before the ocean has a depth of 4000 m and the shelf a depth of 50 m.

The figures show  $R$  for positive values of angular velocity  $\omega$ . For negative values we have from eqn. 4,

$$R(\omega) = R(-\omega^*)^* , \quad (21)$$

where the stars represents complex conjugate. For real values of  $\omega$  plotted here, the real (imaginary) component of  $R$  is symmetric (anti-symmetric) about the origin. Extended into the complex plane the two components have the same symmetries about the imaginary axis.

In the limit of zero angular velocity,  $R$  tends to the value 1.0. Mathematically this is a consequence of eqn. 21. Physically it arises because low angular velocities correspond to very long wavelengths and small velocities. The narrow shelf then acts as a vanishingly small perturbation to the boundary.

As the angular velocity increases, the imaginary component of  $R$  increases linearly but it then shows a rapid oscillation, also reflected in the real component, around an angu-

lar velocities of 12, 36 and 60 radians per day and at similar intervals at higher frequencies.

The previous section showed that friction only has a small effect on the wavenumber on the shelf. Thus we can estimate the wavelengths,  $\lambda$ , using the wave speed for a frictionless shelf,

$$\lambda = 2\pi (gh_2)^{1/2} / \omega. \quad (22)$$

For a depth of 50 m and an angular velocity of 12 radians per day this gives a wavelength of 1002 km, so the shelf is almost exactly one-quarter of a wavelength wide. Similarly for the features at 36, 60 radians per day and higher, the shelf width is approximately 3/4, 5/4 etc wavelengths wide. These equal the classic organ-pipe ratios and imply that we are seeing the effect of resonances of the continental shelf.

It is instructive to plot the real and imaginary components against each other for the same range of  $\omega$ , as has been done in fig. 5. As each resonance is passed the locii form circular features. For the frictionless case ( $\kappa = 0$ ),  $|R|$  always equals one and the locus forms a circle centred on the origin. When friction is present the locii start from the point  $1 + i0$ , and as  $\omega$  increases, they spiral in towards a limiting circle. The figure also shows that as  $\kappa$  increases the radius of the circle becomes smaller, tending to zero as  $\kappa$  becomes very large. Increases in  $\kappa$  also move the centre of the circle in a positive direction along the real axis.

One consequence of this behaviour is that there exists a range of values of  $\kappa$  for which the spirals pass through or very close to the origin. This results in a set of angular velocities  $\omega$  at which there is little or no reflected tidal energy so the incident energy is being almost completely absorbed by the continental shelf. Figures 3 to 6, shows that this occurs near to the resonant frequencies of the system.

In conclusion the results show that continental shelves can resonantly absorb of tidal energy for physically realistic values of the width, depth and friction parameters. Away from resonance most of the incident energy is reflected back into the deep ocean so this further emphasises the importance of resonant shelves. Such a conclusion is consistent with our knowledge of the main tidal dissipation regions of the real ocean; many of which, for example, the Bristol Channel, the Argentinian Shelf and the North-West Australian Shelf, appear to be resonant continental shelves.

#### 4.2.1 Loop Structures

If eqn. 18 is expanded in terms of the real and imaginary components of each variable, it has the form,

$$F(\omega) = \frac{\cos(w + ig) + i(c + id) \sin(w + ig)}{\cos(w + ig) - i(c + id) \sin(w + ig)}. \quad (23)$$

where  $w$ ,  $g$ ,  $c$  and  $d$  are real functions of  $\omega$ . The properties of this equation are discussed in Appendix II and the results help to explain the properties of the loop structures seen in fig. 5.

The basic result obtained is that circular locii are produced whenever  $w$  is a function of  $\omega$  and  $g$ ,  $c$  and  $d$  are constants. In the case of a frictionless shelf, from eqns. 8 and 14 one finds that  $g$  and  $d$  are zero and  $c$  is a constant. In that case Appendix II shows that the function generates circles of unit radius centered on the origin.

If friction is present then circles centered on the real axis are produced in the limit when  $|\omega|$  is large compared to  $\beta_2$ . This arises because in this limit  $g$  and  $c$  tend to constants and  $d$  tends to zero. As friction is increased, then from eqn. 8,  $g$  also increases and from eqn 65, the radius of the loops tends to zero.

However in a sense the loop structure is more fundamental and results from the fact that the functions  $R(\omega)$  and  $A(\omega)$  are analytic functions of  $\omega$ . As a result, if there are no cuts in the complex plane, they can be represented as the sum of the contributions from a set of poles. Thus

$$R(\omega) = \sum_j R_j / (\omega - \omega_j), \quad (24)$$

where  $\omega_j$  is the resonant frequency of the  $j$ 'th pole and  $R_j$  its residue<sup>2</sup>. As discussed in Appendix I, each term of the form  $R_i / (\omega - \omega_j)$  then produces a single loop as  $\omega$  goes from minus to plus infinity, with the width of the resonance, as seen in figs. 3, 4 and 5, depending on the imaginary component of  $\omega_j$ .

## 5 The Complex Plane and Resonances

The above result indicates that the behaviour of the physical system at real values of the angular velocity  $\omega$  is related to poles in the corresponding analytic functions at complex values of  $\omega$ . One way to illustrate this is to consider the response of the continental shelf model to an arbitrary incident wave with a time dependence  $h(t)$ . Using a fourier transform to split this into its various angular velocity components  $h(\omega)$ ,

$$h(\omega) = \frac{1}{2\pi} \int_{-\infty}^{\infty} \exp(i\omega t) h(t) dt. \quad (25)$$

In terms of angular velocity, the wave reflected by the shelf,  $r(\omega)$ , is  $R(\omega)h(\omega)$ . the corresponding function of time is thus,

$$\begin{aligned} r(t) &= \frac{1}{2\pi} \int_{-\infty}^{\infty} \exp(-i\omega t) R(\omega) h(\omega) d\omega \\ &= \frac{1}{2\pi} \int_{-\infty}^{\infty} \int_{-\infty}^{\infty} \exp(-i\omega(t-t')) R(\omega) h(t') dt' d\omega, \end{aligned}$$

<sup>2</sup>If there are cuts in the plane, as discussed in Webb (1982), there is an additional contribution due to the cut which, except near the ends of the cut, is a generally a smooth function.

$$= \frac{1}{2\pi} \int_{-\infty}^{\infty} \int_{-\infty}^{\infty} \exp(-i\omega(t-t')) \sum_i R_i / (\omega - \omega_i) h(t') dt' . \quad (26)$$

But if the imaginary part of  $\omega_i$  is negative then,

$$\int_{-\infty}^{\infty} \exp(-i\omega\tau) R_i / (\omega - \omega_i) d\omega = \begin{cases} 2\pi i \exp(-i\omega_i\tau) R_i & \text{if } \tau > 0, \\ 0 & \text{if } \tau < 0. \end{cases} \quad (27)$$

So,

$$r(t) = \sum_i R_i \int_{-\infty}^t \exp(-i\omega_i(t-t')) h(t') dt' . \quad (28)$$

If the incoming wave is in the form of a very high and narrow pulse arriving at time zero, i.e. in the form of a delta function, then for positive times the outgoing wave has the form,

$$\begin{aligned} r(t) &= \sum_i R_i \int_{-\infty}^t \exp(-i\omega_i(t-t')) \delta(t') dt' , \\ &= \sum_i R_i \exp(-i\omega_i t) . \end{aligned} \quad (29)$$

Thus the resulting reflected wave consists of a number of decaying waves, each having the angular velocity and decay rate of one of the resonant modes of the continental shelf.

### 5.1 The Complex Plane

Another way of illustrating the role of the shelf resonances is to plot quantities in the complex plane. In fig. 7, this is done for the real component of the function  $R(\omega)$  when  $\kappa$  is zero. It shows the region of the complex plane where real component of  $\omega$  is greater than zero and its imaginary component is less than zero.

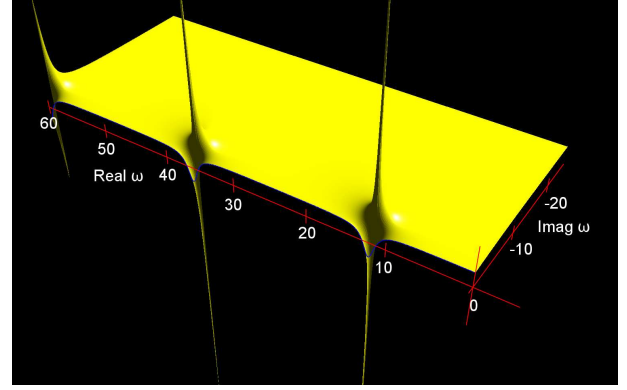
The values plotted along the real axis are the same as those in fig. 3, but the figure now shows that the regions where the real axis values change rapidly are each connected to regions with large positive and negative peaks. The latter are due to the poles, near to each of which the function has the form,

$$R(\omega) = R_i / (\omega - \omega_i) + B(\omega) , \quad (30)$$

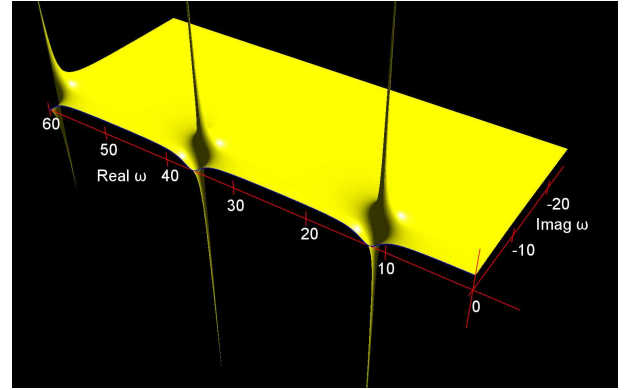
where  $B(\omega)$  is the smooth background contribution from distant poles. As  $\omega$  tends towards  $\omega_i$ , the components of  $R(\omega)$  tend towards plus or minus infinity, the sign depending on the direction of approach.

Figure 8 shows the corresponding result when  $\kappa$  is 0.1. Each of the poles has moved further away from the real axis as a result of which the width of the real axis affected is increased. If,

$$\omega_i = w_i - i\Gamma_i ,$$



**Fig. 7.** The real part of the reflection coefficient  $R$  as an function of complex angular velocity,  $\omega$ , when the friction coefficient,  $\kappa$ , is set to zero. The figure shows the region where the real component of  $\omega$  is greater than zero and the imaginary component is less than zero. The real part of  $R$  has the value 1.0 at the origin and the whole figure is symmetric about the imaginary  $\omega$  axis. The position of the poles are given in table 2.



**Fig. 8.** The amplitude of the reflection coefficient  $R$  as an function of complex angular velocity  $\omega$ , when the friction coefficient,  $\kappa$ , is set to 0.1. The position of the poles are given in table 2.

then, from eqn. 30, on the real axis,

$$R(w) = \frac{R_i((w - w_i) - i\Gamma)}{(w - w_i)^2 + \Gamma^2} + B(w) . \quad (31)$$

The half-width of the region affected is thus equal to the imaginary component of the resonance angular velocity  $\omega_i$ .

### 5.2 The Reflection Coefficient and Resonances

The poles of the reflection coefficient  $R(\omega)$  occur when the denominator of eqn. 18) is zero, i.e. when,

$$\cos(k_2 a) - i(k_1/k_2) \sin(k_2 a) = 0 . \quad (32)$$

Webb (1976) used a Green's Function to show that each pole was due to a decaying shelf mode. A more straightforward

approach is to look for solutions of eqn. 1 with no incident wave. Under these conditions Eqn. 17 becomes,

$$R = A \cos(k_2 a), \quad (33)$$

$$R = i(k_1/k_2)A \sin(k_2 a)$$

This has a solution if,

$$A \cos(k_2 a) = i(k_1/k_2) A \sin(k_2 a). \quad (34)$$

which also implies eqn. 32. It is convenient to rewrite the equation in the form,

$$1 - i(k_1/k_2) \tan(k_2 a) = 0. \quad (35)$$

Then as  $k_1/k_2$  is small, the equation will be satisfied when  $\tan(k_2 a)$  is large, i.e. near one of the poles in the expansion,

$$\tan(z) = \sum_{n=-\infty}^{+\infty} 1/((n+1/2)\pi - z). \quad (36)$$

Thus the  $n$ 'th mode occurs when,

$$1 - i(k_1/k_2)/((n+1/2)\pi - k_2 a) = 0. \quad (37)$$

and near to this pole,  $R(\omega)$  has the form,

$$R(\omega) \approx \frac{1 + i(k_1/k_2)/((n+1/2)\pi - k_2 a)}{1 - i(k_1/k_2)/((n+1/2)\pi - k_2 a)}. \quad (38)$$

Using eqns. 8 and 14 and rearranging,

$$\begin{aligned} R(\omega) &\approx \frac{((n+1/2)\pi - k_2 a) + i(c_2/c_1)}{((n+1/2)\pi - k_2 a) - i(c_2/c_1)}, \\ &\approx \frac{\omega - (n+1/2)\pi\delta_\omega + i\Gamma_s - i\Gamma_d}{\omega - ((n+1/2)\pi\delta_\omega + i\Gamma_s + i\Gamma_d)} \end{aligned} \quad (39)$$

where,

$$\begin{aligned} \delta_\omega &= c_2/a, \\ \Gamma_s &= \beta/2, \quad \Gamma_d = \delta_\omega c_2/c_1, \end{aligned} \quad (40)$$

$\delta_\omega^{-1}$  is the time it takes the wave to cross the shelf. For the  $n$ 'th pole,

$$\omega \approx (n+1/2)\pi\delta_\omega - i\Gamma_s - i\Gamma_d \quad (41)$$

$\Gamma_s$  is the decay rate due to bottom friction on the shelf and  $\Gamma_d$  that due to radiation into the deep ocean.

The above results also show that  $R(\omega)$  can be zero for real values of  $\omega$  (i.e.  $\omega = (n+1/2)\pi\delta_\omega$ ) but only when the two terms  $\Gamma_s$  and  $\Gamma_d$  are equal. All the incident energy is then absorbed by the shelf. Resonant absorption of tidal energy by a continental shelf is thus another example of impedance matching as seen in many other areas of physics.

For the ocean and shelf used for figs 3 to 6,

$$\begin{aligned} h_1 &= 4000 \text{ m.}, & h_2 &= 50 \text{ m.} \\ a &= 250 \text{ km.} \end{aligned} \quad (42)$$

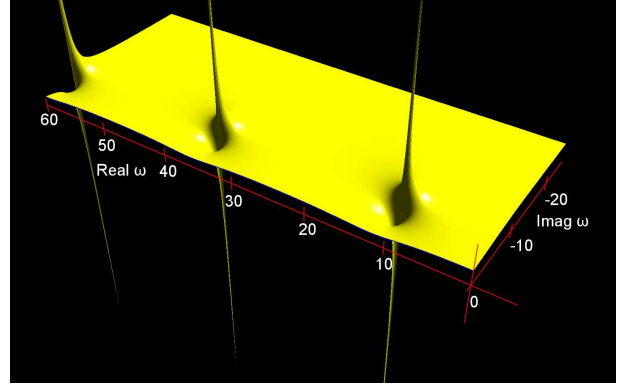


**Fig. 9.** The amplitude of the reflection coefficient  $R$  as an function of complex angular velocity  $\omega$ , when the friction coefficient,  $\kappa$ , is set to 0.5. The position of the poles are given in table 2.

Then,

$$\begin{aligned} c_2/c_1 &= 0.112 \\ \delta &= 1.728 \text{ day}^{-1}, \quad \delta_\omega\pi/2 = 12.02 \text{ day}^{-1}. \end{aligned} \quad (43)$$

Thus the first resonances lies near the semi-diurnal tidal band. If the friction coefficient equals  $10^{-3} \text{ m s}^{-1}$ , then,

$$\begin{aligned} \Gamma_s &= 10^{-5} \text{ s}^{-1} \\ &= 0.864 \text{ day}^{-1} \\ \Gamma_d &= 0.856 \text{ day}^{-1}. \end{aligned} \quad (44)$$

The values of  $\Gamma$  are almost equal, showing that realistic values of depths, shelf widths and bottom friction provide almost perfect matching for the semi-diurnal tides.

### 5.3 Increased Friction

So far we have considered friction coefficients typical of those for a realistic continental shelf. As the friction coefficient  $\kappa$  is increased further, the resonances continue moving away from the real axis away as shown in fig 9 but the the real component of angular velocity reduces until eventually it becomes zero. At this point the resonance meets its complex conjugate with angular velocity  $-\omega^*$ . Additional friction moves the poles along the imaginary axis, one towards the origin and the other towards minus infinity.

The paths of the resonances are shown in fig. 11. Starting from an initial estimate resonances positions were found, following eqn. 30, by fitting the function  $R(\omega)$  at four neighbouring points to the expansion,

$$R(\omega) = A/(\omega - \omega_0) + B\omega + C, \quad (45)$$

where  $A$ ,  $B$ ,  $C$  and  $\omega_0$  are complex and  $\omega_0$  is the new resonance position. This process was iterated until the solution

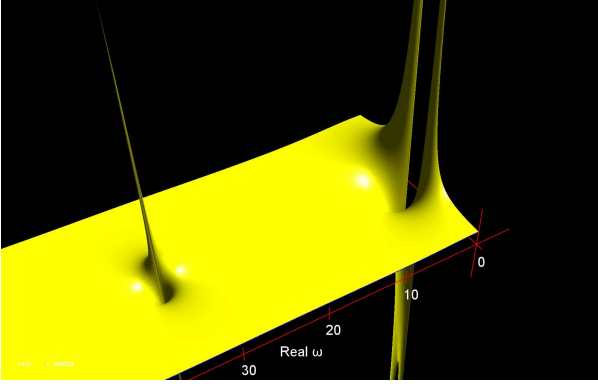


**Fig. 10.** The amplitude of the reflection coefficient  $R$  as an function of complex angular velocity  $\omega$ , when the friction coefficient,  $\kappa$ , is set to 1.3. The position of the poles are given in table 2.

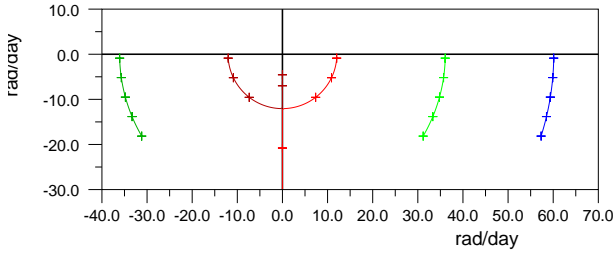


**Fig. 11.** The locii traced out by the lowest order resonances in the complex angular velocity plain as the friction coefficient increases from zero to two. The small crosses plotted at intervals of 0.5.

had converged. This was then used as the starting point for the next value of  $\kappa$ .

An example of the effect of large friction on the function  $R(\omega)$  is shown in fig 10 where  $\kappa$  equals  $1.3 \text{ ms}^{-1}$ . The value is unrealistically high for the real ocean, but there may be shallow regions where a similar value of  $\kappa/h$  is found.

The resonances in fig. 11 appear to follow circular paths up to the point that they reach the imaginary axis. This behaviour is analysed in Appendix 3 where it is shown that the result is exact for the forced problem where there is no radiation damping (discussed below) but is only approximately true for the more general case.

#### 5.4 The Open Boundary

Although the simple 1-D model can be treated analytically, the complexity of real coastlines and topography means that most realistic problems continental shelves have to be solved using 2-D or 3-D numerical models. Such models usually do not include the whole ocean and so an open boundary condition has to be implemented.

**Table 2.** The (complex) angular velocities  $\omega$  of the lowest shelf modes for different values of the friction coefficient  $\kappa$ . When the real component is non-zero, there is a corresponding complex conjugate mode at angular velocity  $-\omega^*$ .

$\kappa$	Mode 1	Mode 2	Mode 3
0.0	( 12.023, -0.859)	( 36.069, -0.859)	( 60.115, -0.859)
0.1	( 11.929, -1.728)	( 36.038, -1.724)	( 60.096, -1.724)
0.5	( 10.874, -5.202)	( 35.704, -5.182)	( 59.897, -5.180)
1.3	( 0.000, -10.623) ( 0.000, -13.681)	( 33.989, -12.096)	( 58.891, -12.093)

In the present problem the key component causing the resonances is the change in depth between the shelf and the deep ocean. As a result the analytic solutions used to construct the figures could have been generated by a numerical model so long as the model included both sufficient horizontal resolution and the change in depth. To correctly represent the effect of the rest of the ocean, the open boundary condition also needs to generate the incoming wave and allow the reflected wave to pass out of the model without interference.

This was straightforward for the present 1-D model but with a 2-D model the radiation part of the boundary condition only works for outgoing waves which are travelling at right angles to the boundary. Given the complications this produces, it is of interest to investigate the effect of removing the radiation part of the boundary condition and imposing just the forced wave at the boundary.

For this case the boundary condition at the coast is as before and, if the wave at the shelf edge has unit amplitude, the boundary condition there becomes,

$$A(\omega) \cos(k_2 a) = 1, \quad (46)$$

where  $A(\omega)$  is the amplitude of the solution on the shelf. It will have poles where,

$$\cos(k_2 a) = 0.$$

Using eqn. 7 to substitute for  $k_2$ , these occur when,

$$\begin{aligned} \frac{\omega a}{c_2} \left(1 + i \frac{\beta_2}{\omega}\right)^{1/2} &= (n + 1/2)\pi, \\ \omega^2 + i\beta_2 \omega - (c_2/a)^2 ((n + 1/2)\pi)^2 &= 0, \end{aligned}$$

where  $\omega$  is the resonant angular velocity and  $n$  is integer. Solving for  $\omega$  and using eqn. 40,

$$\omega = -i\Gamma_s \pm \sqrt{((n+1/2)\pi\delta_\omega)^2 - \Gamma_s^2}. \quad (47)$$

When friction is small, the positive solution is,

$$\omega \approx (n+1/2)\pi\delta_\omega - i\Gamma_s + \dots \quad (48)$$

This differs from eqn. 41 in that the radiation term  $\Gamma_d$  is missing. As this is of similar size to  $\Gamma_s$ , continental shelf models without a radiation condition will significantly underestimate the decay rates of the resonances.

## 6 Discussion

The main aim of this note has been to summarise some previous results and to explore further properties of a 1-D model of continental shelf resonances. This has been done in order to provide a background to studies with more realistic models of the tides and other barotropic waves in the ocean. It has been shown that in the absence of a coastline, a large fraction of the incident wave energy can propagate from the deep ocean onto the shelf.

The situation is very different when there is a nearby coastline, for then most of the energy is reflected unless the shelf is near resonance. The results also confirm that resonant shelves can absorb all of the incident tidal energy and that this is possible with physically realistic values of the ocean and shelf depths, and the shelf width and friction parameter.

The properties of the reflection coefficient  $R$  have been investigated and it has been shown that the resonances are associated with poles in the complex angular velocity plane, the real and imaginary coordinate of the pole corresponding to the frequency and decay rate of the corresponding shelf mode. When friction is increased the poles move away from the real axis but even with zero friction they lie just off the real axis, the imaginary component corresponding to the decay of the shelf mode due to radiation into the deep ocean.

It has also been shown that the real and imaginary components of  $R$ , when plotted against each other while  $\omega$  is varied, generate loop structures that become circles in the limit of zero friction or large  $\omega$ . Such loops are shown to be a consequence of the analytic form of the mathematical functions involved, each resonance pole producing one such loop. As a result of these properties, the presence of similar loops should be a useful indication of the presence of nearby resonances in both model results and data from the real ocean.

### Appendix 1. Loci in the Complex Plane

When the real and imaginary components of quantities such as the reflection coefficient  $R(\omega)$  are plotted against each other then, as  $\omega$  is varied, they show a series of positive, anticlockwise, loops which may be almost circular in form.

This behaviour is a consequence of the fact that linear systems, such as the one described by eqn. 1, have solutions which are analytic in angular velocity space. As a result quantities such as  $R(\omega)$  can be expressed in the form,

$$R(\omega) = \sum_j R_j / (\omega - \omega_j), \quad (49)$$

where the sum is over all the poles of the function. These occur at angular velocities  $\omega_j$  and have residues  $R_j$ .

The contribution of a single pole has the form,

$$C_j(\omega) = R_j / (\omega - \omega_j). \quad (50)$$

Let,

$$\omega_j = W_j - i\Gamma_j, \quad (51)$$

where  $W_j$  and  $\Gamma_j$  are both real. Then,

$$C_j(\omega) = R_j / (\omega - W_j + i\Gamma_j). \quad (52)$$

Let,

$$P_j = -\Gamma_j / (\omega - W_j). \quad (53)$$

Substituting for  $\omega$  and rearranging,

$$C_j(\omega) = R_j / (2i\Gamma_j)(-2iP_j) / (1 - iP_j), \quad (54)$$

$$= R_j / (2i\Gamma_j)(1 - (1 + iP_j) / (1 - iP_j)), \quad (54)$$

$$= R_j / (2i\Gamma_j)(1 - ((1 - P_j^2) + 2iP_j) / (1 + P_j^2)). \quad (55)$$

Let the (real) angle  $u_j$  be defined,

$$\theta_j = 2 \tan^{-1}(P_j) = 2 \tan^{-1}(\Gamma_j / (\omega - W_j)), \quad (56)$$

then using the half angle formula, (Abramowitz & Stegun, 1965, Eqn. 4.3.23),

$$C_j(\omega) = R_j / (2i\Gamma_j)(1 - \exp(i\theta_j)). \quad (57)$$

As  $\omega$  increases from negative to positive infinity, the angle  $\theta_j$  increases from 0 to  $2\pi$  and  $C_j(\omega)$  circles the point  $R_j / (2i\Gamma)$  in a positive (anticlockwise) direction, starting and ending at the origin.

### Appendix 2. The Function $R(\omega)$

In the case of a finite width shelf, the reflection coefficient  $R(\omega)$  (eqn 18) can be written in the form,

$$R(\omega) = \frac{(\cos(w + ig) + i(c + id) \sin(w + ig))}{(\cos(w + ig) - i(c + id) \sin(w + ig))}, \quad (58)$$

where  $w$ ,  $g$ ,  $c$  and  $d$  are all real. Substituting,

$$\cos(w + ig) = \cos(w) \cosh(g) - i \sin(w) \sinh(g),$$

$$\sin(w + ig) = \sin(w) \cosh(g) + i \cos(w) \sinh(g),$$

and simplifying,

$$R(\omega) = \frac{(1 - (c + id) \tanh(g)) + i \tan(w) ((c + id) - \tanh(g))}{(1 + (c + id) \tanh(g)) - i \tan(w) ((c + id) + \tanh(g))}. \quad (59)$$

If,

$$T = \tanh(g),$$

$$S = c + id,$$

then further manipulation gives,

$$R(\omega) = C + D \frac{(1 + iE \tan(w))}{(1 - iE \tan(w))}, \quad (60)$$

where,

$$\begin{aligned} C &= T(1 - S^2)/((1 + ST)(S + T)), \\ D &= S(1 - T^2)/((1 + ST)(S + T)), \\ E &= (S + T)/(1 + ST). \end{aligned}$$

Let,

$$F(\omega) = \frac{(1 + iE \tan(w))}{(1 - iE \tan(w))}. \quad (61)$$

If  $P$  and  $Q$  are the real and imaginary components of  $E$ , then after further manipulation,

$$F(\omega) = -iQ/P + (1 + iQ/P) \frac{1 + iP \tan(w)/(1 + Q \tan(w))}{1 - iP \tan(w)/(1 + Q \tan(w))}. \quad (62)$$

The last term has the same form as the last term in eqn. 54.

Let,

$$\tan(\theta/2) = P \tan(w)/(1 + Q \tan(w)). \quad (63)$$

As  $w$  increases from  $n\pi$  to  $(n+1)\pi$ ,  $\theta$  increases by an angle  $2\pi$ . Using the half-angle formula as before,

$$\begin{aligned} F(w) &= -iQ/P + (1 + iQ/P) \exp(i\theta), \\ R(\omega) &= (C - iDQ/P) + D(1 + iQ/P) \exp(i\theta). \end{aligned} \quad (64)$$

$C$ ,  $D$ ,  $P$  and  $Q$  are independent of  $\omega$ . So as  $\omega$  and thus  $w$  and  $\theta$  vary, the locus of  $R(\omega)$  generates a series of circles centered at  $(C - iDQ/P)$  with radius  $|D(1 + iQ/P)|$ .

If  $d$  is zero, then  $S$ ,  $C$ ,  $D$  and  $E$  have zero imaginary components and  $Q$  is zero. Then,

$$\begin{aligned} C &= \tanh(g)(1 - c^2)/((1 + c \tanh(g))(c + \tanh(g))), \\ D &= c(1 - \tanh(g)^2)/((1 + c \tanh(g))(c + \tanh(g))), \end{aligned} \quad (65)$$

and,

$$R(\omega) = C + D \exp(i\theta). \quad (66)$$

As  $C$  is real, the circles are centered on the real axis. If  $g$  is zero then  $C$  is zero and  $D$  equals one, so the circles are centered on the origin and have unit radius.

### Appendix 3. Path of Poles due to Friction

The forced problem, discussed in section 5.4, has an exact solutions for the position of the poles. Define  $\alpha$  such that,

$$\alpha^2 = ((n + 1/2)\pi\delta_\omega)^2 - \beta^2. \quad (67)$$

If  $\alpha^2$  is positive then, from eqn. 47, the two solutions lie on an circle with radius  $(n + 1/2)\pi\delta_\omega$  centred on the origin. As friction is increased, the poles move towards the negative imaginary axis, reaching it when  $\alpha$  is zero. As friction and  $\beta$  increase further,  $\alpha$  becomes imaginary. The two solutions separate but continue lying on the negative imaginary axis at  $(-i\beta + \alpha)/2$  and  $(-i\beta - \alpha)/2$ .

For the general case, including radiation damping, a higher order solution to Eqn 37 is required. Writing this in the form,

$$(n + 1/2)\pi - k_2 a = -i(k_1/k_2)' \quad (68)$$

Substituting for  $k_1$  and  $k_2$ ,

$$\begin{aligned} (n + 1/2)\pi - (1 + i\beta/\omega)^{1/2} \omega a / c_2 \\ = -i(c_2/c_1)(1 + i\beta/\omega)^{-1/2}. \end{aligned} \quad (69)$$

The term on the right is much smaller than those on the left, so to a first approximation,

$$(1 + i\beta/\omega)^{1/2} \approx (n + 1/2)\pi c_2 / (\omega a).$$

Substituting this approximation on the right of eqn. 69,

$$\begin{aligned} (n + \frac{1}{2})\pi - \frac{\omega a}{c_2} (1 + i\frac{\beta}{\omega})^{1/2} &\approx i\frac{c_2}{c_1} \frac{\omega a}{(n + 1/2)\pi c_2}, \\ \omega(1 + i\frac{\beta}{\omega})^{1/2} &\approx \frac{c_2}{a} (n + \frac{1}{2})\pi - i\frac{c_2}{c_1} \frac{\omega}{(n + 1/2)\pi}. \end{aligned} \quad (70)$$

Squaring both sides,

$$\omega^2 + i\beta\omega - (\frac{c_2}{a})^2 ((n + 1/2)\pi - i\frac{\omega a}{(n + 1/2)\pi c_1})^2 \approx 0.$$

Expanding and dropping the term in  $(c_2/c_1)^2$ ,

$$\omega^2 + i(\beta + \frac{2c_2^2}{c_1 a})\omega - ((n + 1/2)\pi \frac{c_2}{a})^2 \approx 0.$$

Substituting from eqn 40

$$\omega^2 + i2(\Gamma_s + \Gamma_d)\omega - ((n + 1/2)\pi\delta_\omega)^2 \approx 0.$$

with solution,

$$\omega \approx -i(\Gamma_s + \Gamma_d) \pm \sqrt{((n + 1/2)\pi \frac{c_2}{a})^2 - (\Gamma_s + \Gamma_d)^2}. \quad (71)$$

Thus, as long as the ratio  $c_2/c_1$  is small, the resonant frequencies behave in a similar manner to the forced problem.

### References

- Abramowitz, M., and Stegun, I.A.: Handbook of mathematical Functions. Dover Publications, New York, 1965.
- Arbic, B.K., St Laurent, P., Sutherland, G., and Garrett, C.: On the resonance and influence of the tides in Ungava Bay and Hudson Strait. Geophysical Research Letters, 34, 2007.
- Arbic, B.K., Karsten, R.H., and Garrett, C.: On Tidal Resonance in the Global Ocean and the Back-Effect of Coastal Tides upon Open-Ocean Tides. Atmosphere-Ocean, 47 (4), 239-266, 2009.
- Buchwald, V.T.: Resonance of Poincaré waves on a continental shelf. Australian Journal of Marine and Freshwater Research, 31(4), 451-457, 1980.
- Cartwright, D.E. and Ray, R.D.: Tides from Geosat Altimetry. Journal of Geophysical Research, 95 (C9), 3069-3090, 1990.
- Clarke, A.J., and Battisti, D.S.: The effect of continental shelves on tides. Deep Sea Research, 28A (7), 665-682, 1981.

- Das, P., and Middleton, J.H.: Obliquely incident Poincaré waves on a sloping continental shelf. *Journal of Physical Oceanography*, 27 (7), 1274-1285, 1997.
- Duff, G.D.F.: Tidal resonance and tidal barriers in the Bay of Fundy system. *Journal of the Fisheries research Board of Canada*, 27, 1701-1728, 1970.
- Egbert, G.D., and Ray, R.D.: Estimates of  $M_2$  tidal energy dissipation from TOPEX/Poseidon altimeter data. *Journal of Geophysical Research*, 106 (C10), 22475-22502, 2001.
- Egbert, G.D., and Ray, R.D.: Semi-diurnal and diurnal tidal dissipation from TOPEX/Poseidon altimeter data. *Geophysical Research Letters*, 30 (17), 1907, doi:10.1029/2003GL017676, 2003.
- Fong, S.W. and Heaps, N.S.: Note on the quarter-wave tidal resonance in the Bristol Channel. *Institute of Oceanographic Sciences, Report No. 63*, 15p, 1978.
- Greenberg, D.A.: A numerical model investigation of tidal phenomena in the Bay of Fundy and Gulf of Maine. *Marine Geodesy*, 2 (2), 161-187, 1979.
- Heath, R.A.: Resonant period and Q of the Celtic Sea and Bristol Channel. *Estuarine, Coastal and Shelf Science*, 12 (3), 291-301, 1981.
- Huthnance, J.: On shelf-sea resonance with application to Brazilian M3 tides. *Deep Sea Research*, 27A (5), 347-366, 1980.
- Middleton, J.H., and Bode, L.: Poincaré waves obliquely incident to a continental shelf. *Continental Shelf Research*, 7(2), 1274-1285, 1987.
- Miller, G.R.: The flux of tidal energy out of the deep ocean. *Journal of Geophysical Research*, 71, 2485-2489, 1966
- O'Reilly, C. T., R. Solvason, and C. Solomon (2005), Where are the worlds largest tides?, in *BIO Annual Report 2004 in Review*, edited by J. Ryan, pp. 44-46, *Biotechnol. Ind. Org.*, Washington, D. C.
- Webb, D.J.: On the age of the semi-diurnal tide. *Deep-Sea Research*, 20, 847-852, 1973.
- Webb, D.J.: A model of continental-shelf resonances. *Deep-Sea Research*, 25, 1-15, 1976.
- Webb, D.J.: Tides and Tidal energy. *Contemporary Physics*, 23 (5), 419-442, 1982.